Journal of Catalysis **191,** 46–54 (2000)
doi:10.1006/jcat.1999.2798, available online at http://www.idealibrary.com on IDEAL®

The Contribution of Gas-Phase Reactions in the Pt-Catalyzed Conversion of Ethane–Oxygen Mixtures

Marylin C. Huff,* Ioannis P. Androulakis,† John H. Sinfelt,†,[1] and Sebastián C. Reyes†,[2]

*Center for Catalytic Science and Technology, Department of Chemical Engineering, University of Delaware, Newark, Delaware 19716; and †Corporate Research Laboratories, Exxon Research and Engineering Company, Annandale, New Jersey 08801

Received July 6, 1999; revised November 18, 1999; accepted November 19, 1999

This paper presents an analysis of the oxidative dehydrogenation of ethane on platinum-containing monoliths. The purpose of the work is to make a quantitative assessment of the extent to which homogeneous gas-phase reactions contribute to the overall conversion of the ethane. In making the analysis, extensive use is made of kinetic information obtained and compiled by A. M. Dean and associates for elementary homogeneous reaction steps and by L. D. Schmidt and associates for elementary surface reactions. A critical part of the analysis is concerned with accounting for the heat effects and for the reactor temperature gradient resulting therefrom. This is absolutely essential for meeting the objective of this investigation. The rise in temperature as the gases proceed through the reactor is responsible for a very substantial contribution of homogeneous gas-phase reactions in the chemical transformation occurring. One can view the process as a sequential one in which ethane is first oxidized on the platinum surface to CO, CO_2, and H_2O in the front region of the monolith. The formation of these products causes a substantial temperature increase that drives the dehydrogenation of ethane to ethylene (and acetylene) in the gas phase. The heat required to sustain these endothermic reactions in the tail end of the reaction zone is supplied by exothermic gas-phase oxidation reactions that form additional H_2O and CO. Overall, the system can be viewed as one in which the catalyst initiates gas-phase chemistry through the acceleration of exothermic reactions at the front of the reactor which increase the downstream temperature to the point where gas-phase reactions occur readily.

1. INTRODUCTION

For a long time it has been recognized that the chemical transformations occurring in certain high-temperature processes based on heterogeneous catalysis may involve homogeneous gas-phase reactions in addition to surface-catalyzed reactions. An area of much current interest, in which this possibility must be considered, is the catalytic oxidation of simple alkanes. Temperatures in the range 850–1050°C are commonly experienced in the reactors used for such oxidations, and at these temperatures the rates of homogeneous gas-phase reactions can become high enough to make a significant contribution in the conversion of reactants to products.

In recent years the pioneering research of Professor L. Schmidt and students at the University of Minnesota on hydrocarbon oxidation has attracted much attention (1–5). These investigators have employed ceramic foam monoliths incorporating small amounts of metals such as platinum and rhodium as the active catalyst components. The reaction times required for complete conversion of the reactants are only a few milliseconds and reactor temperatures in excess of 800°C are commonly observed. The approach is similar to that which has long been used in Ostwald's classic process for the oxidation of ammonia to nitric oxide in the commercial production of nitric acid (6). The catalysts in ammonia oxidation are platinum or platinum–rhodium gauzes, and reaction times are typically a few tenths of a millisecond at temperatures in the range 750–950°C (7).

In the oxidation of hydrocarbons with the monoliths, a quantitative assessment of the extent to which homogeneous gas-phase reactions contribute to the overall conversion of the reactants involves the consideration of rates of many different reaction steps and a careful analysis of the heat effects associated with the reactions. The latter, of course, is necessary for the determination of reactor temperature profiles. In view of the complexity of the matter, one might well be skeptical about the reliability of an assessment of the extent of participation of gas-phase chemistry in the process.

In recent years, however it has become increasingly evident that the efforts of Dean and associates to obtain a comprehensive understanding of the kinetics of elementary homogeneous gas-phase reactions of species of the kind observed in the oxidation of hydrocarbons (at temperatures covering the range actually employed in the oxidations) have been very successful (8–10). Moreover, the work of Schmidt and associates resulting in a kinetic description of the pertinent elementary surface reactions in hydrocarbon oxidation has been similarly successful (2, 3, 5).

[1] Senior Scientific Advisor Emeritus.

[2] To whom correspondence should be addressed. Fax: (908) 730-3198. E-mail: screyes@erenj.com.

0021-9517/00 $35.00

These two sources of valuable kinetic information provide a basis for calculating product yields in hydrocarbon oxidation by a standard integration procedure in which one calculates rates of reactions and rates of heat release to obtain concentration and temperature profiles along the reactor. The yields of the various products obtained from such a calculation, and an estimate of the temperature at the reactor outlet, can be compared with experimental data. This provides an indication of how well the kinetic information can be combined to predict the observed results. If a good agreement is obtained, one has a reasonable basis for drawing a conclusion about the extent of participation of gas-phase chemistry in the formation of the reaction products.

In the partial oxidation of methane to synthesis gas ($CO + H_2$) with a rhodium-containing monolith, it appears that surface reactions can account for the observed product yields without any significant participation of gas-phase reactions, as was originally concluded by the Schmidt group at Minnesota (2, 3). For a platinum-containing monolith, which exhibits a lower selectivity to CO and H_2 because of the greater rate of formation of H_2O at the surface (2, 3), one might be less certain that gas-phase reactions do not play a role. The high rate of heat release associated with the formation of H_2O leads to significantly higher reactor temperatures than are observed with the rhodium-containing monolith, thus increasing the possible involvement of gas-phase reactions.

The possibility that gas-phase chemistry plays a role is even greater in the partial oxidation of ethane with a platinum-containing monolith (10). Data on product yields in this system were originally reported by Huff and Schmidt (4), with further work being reported by Huff and Schmidt (5), Witt and Schmidt (11), and Flick and Huff (12). In this system, ethylene is an important product, and significant formation of acetylene is also observed. Consequently, the term *oxidative dehydrogenation* is often used in referring to the process. Additional data for the system are reported in the present paper. The new data cover a range of variables (C_2H_6/O_2 ratio, temperature, conversion) that provide a good test of the ability of the available kinetic information to predict what is observed. In the present paper we show the results of our use of the kinetic information to make such predictions and to make a quantitative assessment of the contribution of gas-phase chemistry in the overall conversion of ethane–oxygen mixtures.

2. EXPERIMENTS

The reactor used for these experiments is described in detail elsewhere (1, 4, 12). The feed is a room temperature mixture of ethane, oxygen, and nitrogen on the fuel-rich side of the flammability limits. In the particular examples described in this paper, the reactants enter the catalytic foam monolith at a pressure of 1.2 atm and a flow rate of 2 slpm. The monolith is a low-surface-area α-Al_2O_3 and has a porosity of about 84% and dimensions of 1.8 cm in diameter and 1 cm in length. The average diameter of the monolith flow channels is about 420 μm. The channel walls are coated with 5.88 wt% Pt. The reactor is insulated axially and radially to minimize heat losses. The active monolith catalyst is sandwiched between two platinum-free monoliths that act as heat shields that reduce upstream and downstream radiation. These inactive monoliths also serve to better distribute the feed over the cross-sectional area of the platinum-containing one. As a result of axial heat conduction from the hot reaction zone, the feed enters the face of the active monolith at a temperature of about 300°C. The external surface of the reactor tube is wrapped with an alumina cloth to minimize heat losses to the surrounding environment. A thermocouple placed between the active monolith and the back radiation shield records the temperature of the outlet stream. This catalyst exit temperature is the experimentally reported value. The composition of the outlet stream is measured by standard analytical methods.

3. REACTOR CONCENTRATION AND TEMPERATURE PROFILES

Our treatment of this matter consists of a one-dimensional plug-flow analysis in which changes in composition (gas and surface) and temperature are described along the axial distance in the monolith. The calculation of the temperature profile is extremely important because of limitations in experimentally measuring the very large temperature variations that occur within millimeter distances. The mass and heat conservation equations are integrated along a single monolith channel (radius r_o) within which surface and gas-phase reactions take place. It is generally accepted that the rates of mass transfer of species between the gas phase and the catalyst surface are rapid compared with their corresponding rates of reaction in each respective phase. The differential equations describing mass conservation in the gaseous stream can be written as

$$\frac{d\omega_i}{dz} = \frac{1}{\rho_o u_o}\left(\sum_{j=1}^{G} R_{ij} + \frac{2}{r_0}\sum_{k=1}^{S} R_{ik}\right), \qquad [1]$$

$$\omega_i(0) = \omega_{i0},\ i = 1, \ldots, N.$$

In these equations, ω_i is the mass fraction of species i, z is the axial monolith distance, ρ_o is the inlet density, and u_0 is the inlet velocity through the monolith channels. R_{ij} and R_{ik} are the rates of reaction of the ith species in the gas-phase reaction j and the surface reaction k, respectively. N is the total number of gaseous species and G and S are the numbers of reactions in the gas phase and on the catalyst surface, respectively. As described later, the numerical values of N, G, and S are 115, 447, and 18, respectively. An

energy balance, which assumes rapid thermal equilibration between the catalyst surface and the surrounding gas phase, leads to the following differential equation for the reactor temperature:

$$\frac{dT}{dz} = \frac{\alpha}{\rho_o u_o C_p} \sum_{i=1}^{N} H_i \left(\sum_{j=1}^{G} R_{ij} + \frac{2}{r_0} \sum_{k=1}^{S} R_{ik} \right), \quad T(0) = T_0. \tag{2}$$

Here, C_p is the heat capacity of the reacting mixture, H_i is the enthalpy of the ith species, and α is an adjustable parameter that quantifies the extent of axial and radial heat losses with $\alpha = 1$ for purely adiabatic operation. This phenomenological description of the heat losses was found to be adequate for the purposes of this work. The parameter α was chosen to give good agreement between calculated and measured temperatures for the entire body of data. With the use of a single value of 0.75 for α, the calculated and experimental values at the reactor outlet always agreed within 10%, and generally the agreement was much better (in the range 1.5 to 5%). The more rigorous approach of solving the differential equations governing the heat conduction and radiation mechanisms within the active monolith and the surrounding shields would severely increase the mathematical complexity of the model. The fact that the parameter α is not very different from one adds credibility to the approach we have taken here.

The time taken for the reacting mixture to reach the axial position z is obtained by integrating the equation

$$\frac{dt}{dz} = \frac{\rho}{\rho_o u_o}, \quad t(0) = 0. \tag{3}$$

This equation arises from a simple mass conservation relationship [$\rho_0 u_0 = \rho(z) u(z)$] that essentially quantifies the changes in velocity that result from temperature rise and molar expansion. Thus, when the temperature (T_0) and the mass fractions (ω_{io}) of the feed components are specified, the integration of Eqs. [1]–[3] determines the gas composition and the temperature as a function of the reactor distance and corresponding residence time. The details of the gas-phase (R_{ij}) and surface (R_{ik}) reactions are described in the following sections.

3.1. Kinetics of the Gas-Phase Reactions

One of the key objectives of the present study is to identify which reactions contribute to the oxidative dehydrogenation of ethane on platinum-containing monoliths. The experiments indicate that oxygen is always completely consumed by the reactions and that ethane conversion is also very high. The main products measured at the reactor outlet are C_2H_4, C_2H_2, CH_4, CO, H_2, CO_2, and H_2O. As shown later, these species are exactly those that are most abundantly produced by gas-phase reactions when mixtures of ethane and oxygen are exposed to temperatures of the order of 800°C (see Fig. 1). Moreover, the time taken for these gas-phase reactions to occur is very similar to the reaction times employed in the catalytic experiments with the monoliths. These findings strongly suggest that gas-phase pathways can be involved in the reactions of ethane–oxygen mixtures.

In our assessment of the contribution of such pathways, the kinetics of the elementary steps are taken from the work of Dean and associates (10). The specific steps involve free radical intermediates and are described in a recent publication by Mims *et al.* (10). The reaction steps were used by these workers to account for secondary reactions of ethylene in an oxidative environment. The reaction network is ideally suited to the purposes of our study because it was derived under conditions of composition and temperature that are very similar to those prevailing in the present experiments. We have also very recently used this network to study C_2 yield enhancements in the oxidative coupling of methane by controlled oxygen addition and product removal strategies (13). The network consists of 115 species that participate in 447 reversible reactions. The Chemkin-II package (14) is used to keep track of these reactions and to determine the physicochemical properties of the reacting mixture.

3.2. Kinetics of the Surface Reactions

In accounting for the contribution of surface reactions in the overall transformation of ethane, it is convenient to consider the transformation to consist of two major parts: (a) an irreversible dissociative chemisorption of ethane leading to the formation of surface hydrogen atoms and carbon atoms, and (b) the reactions of the latter species with chemisorbed oxygen to yield products. In the present work, the kinetics of the reaction steps constituting part b have simply been taken from the work of Schmidt and associates referred to earlier (2, 3). The kinetics were used by these workers in their study of synthesis gas production from methane and oxygen on platinum-containing monoliths at pressures and temperatures similar to those of the present ethane and oxygen experiments. These kinetic parameters are listed in Table 1 (steps 1–17). They are directly used here with only one minor modification: the original kinetic parameters of reactions 1–4 were modified to reflect explicit second-order kinetics instead of the pseudo-first-order kinetics used by Hickman and Schmidt (2, 3).

For part a, the dissociative chemisorption of ethane to produce carbon on the surface presumably proceeds through a sequence of very rapid dehydrogenation steps. In a steady-state situation, the rate of formation of surface carbon atoms can simply be taken to be two times the rate of the initial step in the chemisorption of ethane and, for simplicity, represented as a single step in the analysis. For the purposes of the present investigation, this representation is

TABLE 1

Surface Reactions for Methane and Oxygen on Platinum-Containing Monoliths (2, 3)

	Reaction step	k_0 (s^{-1} or $Torr^{-1}\ s^{-1}$)	E_a (kcal/mol)
1	$H_2(g) + S^* - S^* \xrightarrow{k_{aH}} 2H^*$	$7.1 \times 10^2\sqrt{298/T}$ [a]	0
2	$2H^* \xrightarrow{k_{dH}} H_2(g) + S^* - S^*$	4×10^{13} [a]	18.0
3	$O_2(g) + X^* - X^* \xrightarrow{k_{aO}} 2O^*$	$4.4 \times 10^1\sqrt{298/T}$ [a]	0
4	$2O^* \xrightarrow{k_{dO}} O_2(g) + X^* - X^*$	15.7×10^{13} [a]	52.0
5	$H_2O(g) + S^* \xrightarrow{k_{aH_2O}} H_2O^*$	$5 \times 10^4\sqrt{298/T}$	0
6	$H_2O^* \xrightarrow{k_{dH_2O}} H_2O(g) + S^*$	1×10^{13}	10.8
7	$CO(g) + S^* \xrightarrow{k_{aCO}} CO^*$	$3.21 \times 10^5\sqrt{298/T}$	0
8	$CO^* \xrightarrow{k_{dCO}} CO(g) + S^*$	1×10^{13}	30.0
9	$CO^* + O^* \xrightarrow{k_{dCO_2}} CO_2(g) + S^* + X^*$	1×10^{15}	24.0
10	$H^* + O^* \xrightarrow{k_1} OH^* + X^*$	1×10^{15}	2.5
11	$OH^* + X^* \xrightarrow{k_{-1}} H^* + O^*$	1×10^8	5.0
12	$H^* + OH^* \xrightarrow{k_2} H_2O^* + S^*$	9×10^{16}	15.0
13	$H_2O^* + S^* \xrightarrow{k_{-2}} H^* + OH^*$	1.8×10^{13}	37.0
14	$2OH^* + X^* \xrightarrow{k_3} H_2O^* + O^* + S^*$	1×10^{15}	12.3
15	$C^* + O^* \xrightarrow{k_4} CO^* + X^*$	5×10^{13}	15.0
16	$CO^* + X^* \xrightarrow{k_{-4}} C^* + O^*$	1×10^{11}	44.0
17	$CH_4(g) + S^* \xrightarrow{k_{am}} C^* + 4H^*$	5×10^4	10.3
18	$C_2H_6(g) + S^* \xrightarrow{k} 2C^* + 6H^*$	3×10^5 [b]	4.6[b]

[a] Kinetic parameters for these reactions were modified to reflect second-order kinetics instead of their original first-order values.

[b] From this work.

adequate and again is similar to that adopted by Schmidt and associates for the oxidation of methane (2, 3) and in part for the oxidation of ethane (5). It differs from that of Schmidt and associates in the case of ethane oxidation in that it does not include a parallel pathway in which ethane chemisorption proceeds via interaction with chemisorbed oxygen (5), a process referred to as oxygen-assisted dissociative adsorption. The inclusion of such a parallel pathway increases the complexity of the analysis and introduces more parameters into the description of the system. Since we found that the inclusion of the parallel pathway did not materially affect the results or conclusions in this investigation, we chose not to include it in the interest of simplicity.

If we represent the rate of chemisorption of ethane by the expression.

$$r = k \cdot P_{C_2H_6} \cdot \theta_s, \qquad [4]$$

where $P_{C_2H_6}$ is the ethane pressure, θ_s is the fraction of bare surface sites S*, and k is a rate constant, we note that θ_s is generally very small. The surface is heavily covered with either CO or C (see Fig. 5). Coverage by CO is very high in the initial stages of the reaction. However, by the time that 10% of the ethane is converted (about 1–2 ms), the CO has been almost completely replaced by C. Thus, a major part of the overall reaction occurs after the surface is covered very heavily with carbon. Since the rate of formation of carbon on the surface can be accounted for readily as if the process occurred in a single step, the problem of assigning the contribution of surface reactions in ethane oxidation becomes one of applying the kinetics of Schmidt and associates to part b of the overall transformation defined in the previous paragraph. Since this source of kinetic information has been found to be quite reliable, one has confidence in using the kinetics to make a quantitative assessment of the extent to which surface reactions contribute to the overall conversion of the ethane.

Our analysis indicates that the ethylene, acetylene, and methane produced in the system can be attributed satisfactorily to reactions occurring in the gas phase. Although ethylene and acetylene may be formed on the surface in the course of the dissociative chemisorption of ethane, their rates of desorption from the surface do not compete favorably with the rates of subsequent surface steps involving further dissociation of carbon–hydrogen bonds or the scission of carbon–carbon bonds. These latter steps are the rapid steps already referred to in carbon formation on the surface. Moreover, the formation of methane from monocarbon species on the surface does not compete favorably with the reactions of these surface species with oxygen. Thus, the hydrocarbon products of ethane oxidation are accounted for exclusively by gas-phase reactions.

In the reaction steps listed in Table 1, the surface species are H*, O*, OH*, C*, CO*, and H_2O*. In our analysis, we did not consider the transfer of radicals between the catalyst surface and the gas phase. These effects could be readily implemented in our computer models but this was not found to be necessary to rationalize the data. Mass balances equating the rates of formation and disappearance of these species on the surface lead to six algebraic relationships that are simultaneously solved with Eqs. [1]–[3] to determine the corresponding surface coverages at each position along the monolith. Consistent with the work of Hickman and Schmidt (2, 3), the platinum surface was described by two types of sites: oxygen chemisorption sites (X*) and sites where all the other species could adsorb competitively (S*). Transport of radicals between the catalyst surface and the surrounding gas phase was not included. Thus, the coupling between the gas-phase and surface steps occurs only through the following molecular species: H_2, O_2, H_2O, CO, CO_2, CH_4, C_2H_6.

3.3. Procedure for Estimating Certain Unknown Parameters

As we have already pointed out, our calculations of the extents of conversion of ethane to various reaction products have been based on many kinetic parameters obtained from

the literature. Nevertheless, estimates of a few parameters have been made from the data reported in the present investigation. The only estimate of real importance is that of the parameter α accounting for the heat loss from the reaction zone. The other estimates were for the preexponential factor and activation energy for the step producing surface carbon atoms from ethane and for the preexponential factors for reactions 1–4 in Table 1. These estimates of reaction rate parameters did not lead to predictions of results significantly different from those obtained using the kinetics of Schmidt and associates for these steps (2, 3, 5). The estimates were made simply because of differences from the Schmidt group regarding the formal representations of the kinetic expressions for the rates, rather than the magnitude of the rates.

The data in the present investigation were obtained in six experiments in which variations in the C_2H_6/O_2 ratio (1.2, 1.5, and 1.8) and the amount of N_2 dilution (20 and 50%) produced substantial changes in ethane conversions, selectivities, and reactor temperatures. A formal procedure was developed to determine how well the experimental results could be calculated from the kinetics of the many steps considered in the analysis. The procedure minimized the sum of differences between experimental and calculated values at the reactor outlet:

$$F = \sum_{r=1}^{N_e} \sum_{s=1}^{N_q} \left\| Y_{rs}^{exp} - Y_{rs}^{cal} \right\|. \qquad [5]$$

In the present case, nine (N_q) experimental and calculated quantities (ethane conversion, outlet reactor temperature, and selectivities to C_2H_4, C_2H_2, CH_4, CO, CO_2, H_2, and H_2O) were compared for each of six (N_e) experiments. Mathematically, the solution of the differential-algebraic system was carried out with DDASSL (15) and the minimization problem was solved with a direct search method (Simplex, NAG Fortran Library) which does not require the calculation of numerical derivatives (16). This method helped minimize the number of times the modeling equations needed to be solved to provide the calculated values at the reactor exit. The parameters mentioned in the previous paragraph were the only parameters determined by this minimization. Despite the nonlinear nature of the modeling equations, the minimization of the objective function F consistently led to the same set of parameters when different initial guesses were used. Although it cannot be proved that such a minimum is a global one, the solution appears to be of very good quality and leads to a set of parameters that have meaningful interpretation in the context of the physical problem being analyzed here.

4. RESULTS AND DISCUSSION

Prior to discussing the results on the oxidation of ethane on the platinum-containing monolith, it is instructive to present a simulation where only gas-phase reactions are considered along the monolith channels. The goal of this simulation is to illustrate how significant the rates of the gas-phase reactions can be under the conditions under which the catalyzed experiments are carried out. These results are shown in Fig. 1 for an inlet temperature of 800°C; temperatures greater than 800°C are commonly observed in ethane oxidation experiments. This figure shows the partial pressures of the main species as the reacting mixture traverses the length of the monolith. By making use of Eq. [3], the abscissa is expressed here as a contact time to put the results on the same basis as those observed in the catalyzed experiments. The variation of partial pressures with time is typical of gas-phase oxidation reactions in which an initially slow induction period is followed by the rapid consumption of reactants and formation of products. In this particular example, the reactants are converted almost completely in about 6 ms and no discernible reaction takes place beyond about 9 ms. The main products of the reactions are exactly those that are measured in the catalyzed experiments and they also form within contact times of a few milliseconds. The results in Fig. 1 strongly suggest that gas-phase reactions can occur with high rates under the conditions of the catalyzed experiments, and consequently their possible contribution to the observed product yields should not be neglected in the analysis.

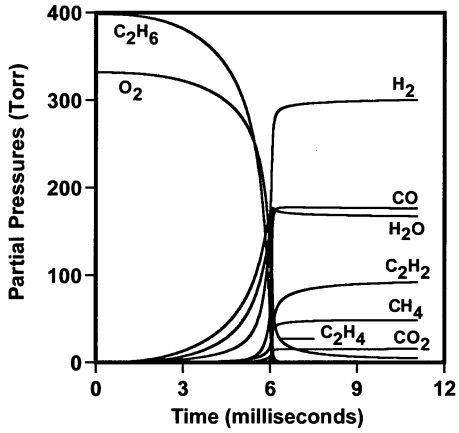

FIG. 1. Partial pressures as a function of contact time. The curves are calculations for gas-phase reactions only (2 slpm, 1.2 atm, $C_2H_6/O_2 = 1.2$, 20% nitrogen dilution, inlet temperature of 800°C).

We now turn to the catalytic experiments and include both surface and gas-phase reactions in the analysis of the data. The results are summarized in Table 2 in tabular form and are also displayed in Fig. 2 as a parity plot. They directly compare the measured and calculated values for the six experiments analyzed in this paper. The agreement is very good. The calculated values correctly follow the experimental trends in conversion, temperature, and product selectivities when the amounts of oxygen and nitrogen in the feed are varied over a wide range. The parameter

TABLE 2

Comparison of Measured and Calculated Values for the Oxidative Dehydrogenation of Ethane over a 5.88 wt% Pt/α-Al_2O_3 Foam Monolith

	$C_2H_6/O_2=1.2$		$C_2H_6/O_2=1.5$		$C_2H_6/O_2=1.8$	
	Exp.	Calc.	Exp.	Calc.	Exp.	Calc.
a. 2 slpm, 1.2 atm, 20% nitrogen dilution						
Temperature (°C)	1052	1125	978	961	900	882
C_2H_6 conv. (%)	98.4	99.8	88.6	94.5	76.4	77.9
C_2H_2 selec. (%)	9.6	10.0	2.9	1.3	0.8	0.4
C_2H_4 selec. (%)	32.1	38.1	54.2	60.9	61.9	66.7
CH_4 selec. (%)	13.0	9.8	8.3	5.6	5.3	3.4
CO selec. (%)	41.3	38.8	25.7	29.5	19.7	26.8
CO_2 selec. (%)	3.3	3.2	6.2	2.7	9.2	2.7
H_2O selec. (%)	23.9	27.6	22.4	25.0	25.2	26.2
H_2 selec. (%)	38.1	32.3	29.5	28.5	25.8	26.2
b. 2 slpm, 1.2 atm, 50% nitrogen dilution						
Temperature (°C)	963	998	892	883	857	841
C_2H_6 conv. (%)	94.5	98.2	80.2	82.4	59.6	62.8
C_2H_2 selec. (%)	4.8	2.3	1.3	0.4	0.3	0.1
C_2H_4 selec. (%)	43.0	51.1	56.2	62.0	60.3	62.1
CH_4 selec. (%)	8.1	6.0	5.0	2.9	3.2	1.8
CO selec. (%)	38.5	37.6	32.1	31.9	28.2	32.8
CO_2 selec. (%)	3.0	3.1	2.5	2.9	4.9	3.1
H_2O selec. (%)	29.8	29.1	31.3	29.1	35.0	32.2
H_2 selec. (%)	25.8	29.8	19.5	26.9	16.5	24.8

estimation analysis indicates that about 25% of the heat released by the reactions is lost into the surrounding environment (i.e., $\alpha = 0.75$). Some of this heat is responsible for bringing the reactants from room temperature up to about 300°C at the entrance of the platinum-containing monolith. Also, the present analysis indicates that the kinetics of ethane dissociation are characterized by an activation energy of 4.6 kcal/mol and a preexponential factor of $3 \times 10^5\ s^{-1}$ as shown in Table 1. The finding of an activation energy lower than that observed for methane is not at all unreasonable (2, 3).

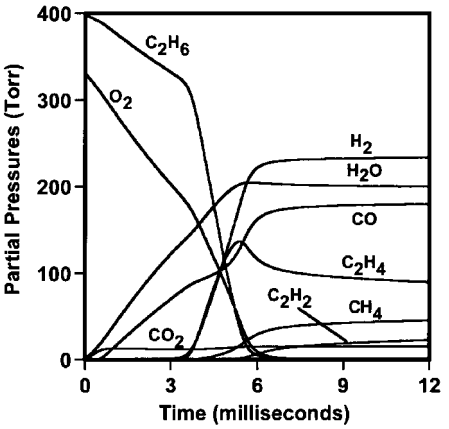

FIG. 3. Partial pressures of main products as a function of contact time. The curves are predictions for $C_2H_6/O_2 = 1.2$ and 20% nitrogen dilution (2 slpm, 1.2 atm, 5.88 wt% Pt/α-Al_2O_3).

Further insight can be obtained by examining the calculated effects of reaction time. Under the conditions of the first experiment as an illustration ($C_2H_6/O_2 = 1.2$, 20% N_2), Figs. 3–5 display the effects on partial pressures, temperatures, and surface coverages. The times can be converted to distances along the monolith. In this particular example, the time taken for the mixture to traverse the length of the monolith is about 12 ms. The flattening of the pressure and temperature profiles in Figs. 3 and 4 at times longer than about 6 ms indicates that reactions are no longer occurring. The calculations also indicate that the velocity of the mixture at the outlet of the reactor is about 4 times that at the entrance to the active monolith. The increase in temperature (300 to 1125°C) plays a greater role (~144%) than the volume expansion due to reaction (~63%) in accelerating the gases along the monolith channels.

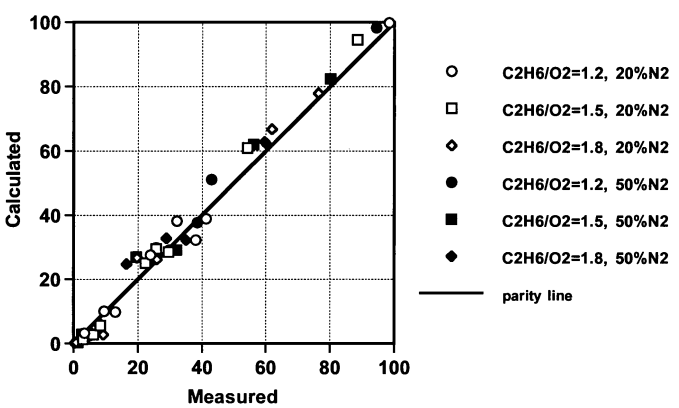

FIG. 2. Parity plot comparing calculated ethane conversion and selectivities (C_2H_2, C_2H_4, CH_4, CO, CO_2, H_2O, H_2) with the experimental values for various C_2H_6/O_2 ratios and levels of nitrogen dilution (2 slpm, 1.2 atm, 5.88 wt% Pt/α-Al_2O_3).

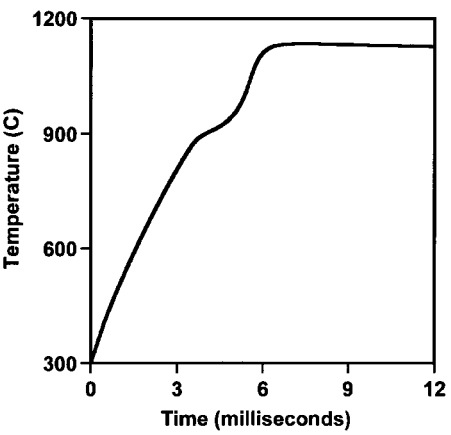

FIG. 4. Reactor temperature as a function of contact time. Calculation for $C_2H_6/O_2 = 1.2$ and 20% nitrogen dilution (2 slpm, 1.2 atm, 5.88 wt% Pt/α-Al_2O_3).

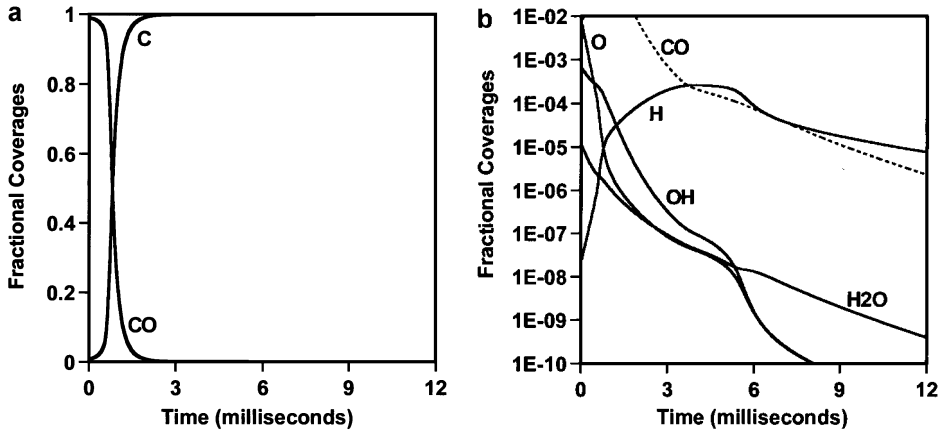

FIG. 5. (a) Surface coverages as a function of contact time. The curves are calculations for $C_2H_6/O_2 = 1.2$ and 20% nitrogen dilution (2 slpm, 1.2 atm, 5.88 wt% Pt/α-Al_2O_3). (a) C and CO. (b) O, H, OH, and H_2O.

Figure 3 shows that reactions begin as soon as the reactants enter the catalytic monolith. As ethane and oxygen begin to be consumed, only CO_2 and H_2O appear initially as reaction products. Since in that region of the monolith the temperature is still relatively low (Fig. 4), these products arise exclusively from surface-catalyzed reactions. Then, as the temperature continues to increase due to the heat released by the reactions, CO is able to desorb from the catalyst surface and consequently appears as a reaction product. At this point, the catalytic production of CO_2 ceases. As the mixture advances further into the monolith, a transition region begins at a contact time of about 4 ms. This transition is evidenced by a change in slope in the partial pressures of ethane and oxygen occurring when the reactor temperature reaches about 850°C. Beyond this point, both ethylene and hydrogen appear as reaction products and some methane also begins to form. H_2O and CO continue to be produced, further raising the temperature to a level at which the dehydrogenation of ethylene to acetylene occurs readily. In addition to the variation in partial pressures and temperature with time, it is instructive to examine the concurrent changes in the concentrations of the adsorbed species. Figure 5a shows that the dominant species on the surface are CO and C. As shown in Fig. 5b, the coverage by other species is always much smaller. In the front region of the monolith, the platinum surface is mostly covered with CO but as the temperature rises, the CO coverage decreases and the C coverage increases. We note that the surface production of CO and H_2O is still very significant past about 3 ms, even though by that time the surface is highly covered by C.

The transition in partial pressures and temperature profiles observed in Figs. 3 and 4 strongly suggests that gas-phase reactions are contributing in the conversion of ethane and oxygen when the temperature exceeds about 850°C. According to our analysis, the formation of ethylene, acetylene, and methane can be accounted for solely by homogeneous gas-phase reactions. The formation of CO, CO_2, H_2, and H_2O can, however, occur either on the surface or on the gas phase. From our analysis, we can determine to what extents surface reactions and gas-phase reactions contribute to the disappearance of reactants and the formation of products. Such calculations are summarized in Fig. 6. This figure plots the rates of reaction of the main species at each position along the monolith. Note that distance was chosen here instead of contact time to avoid the visual distortion of the areas under the curves that would occur due to the acceleration of the gases driven by the temperature rise and by the molar expansion due to reactions. By calculating the areas under the curves, we determine the extents to which surface reactions and gas-phase reactions contribute to the formation or disappearance of the various species.

Figure 6 clearly shows that ethane is consumed first by reactions on the catalyst surface. However, this is subsequently overshadowed by the contribution of reactions occurring in the gas phase (80%). There is an intermediate region where both gas-phase and surface reactions simultaneously contribute to ethane conversion. The relative contributions from the gas phase and the surface can also be seen from the partial pressure profiles plotted in Fig. 3: the ethane pressure falls about 20% prior to the transition that signals the emergence of the gas-phase chemistry. Oxygen, on the other hand, is consumed slightly more by surface (55%) than by gas-phase reactions. Hydrogen is produced predominantly in the gas phase (90%) by dehydrogenation reactions of ethane and ethylene. Interestingly, hydrogen is not produced in the early stages of the reaction but instead appears when the surface is heavily covered by C, when the temperature is very high, and when the gas-phase processes are dominant. This figure also shows that, although the surface reactions produce the carbon monoxide formed in the early stages of reaction, an equal amount is formed later by gas-phase processes. Similarly, carbon

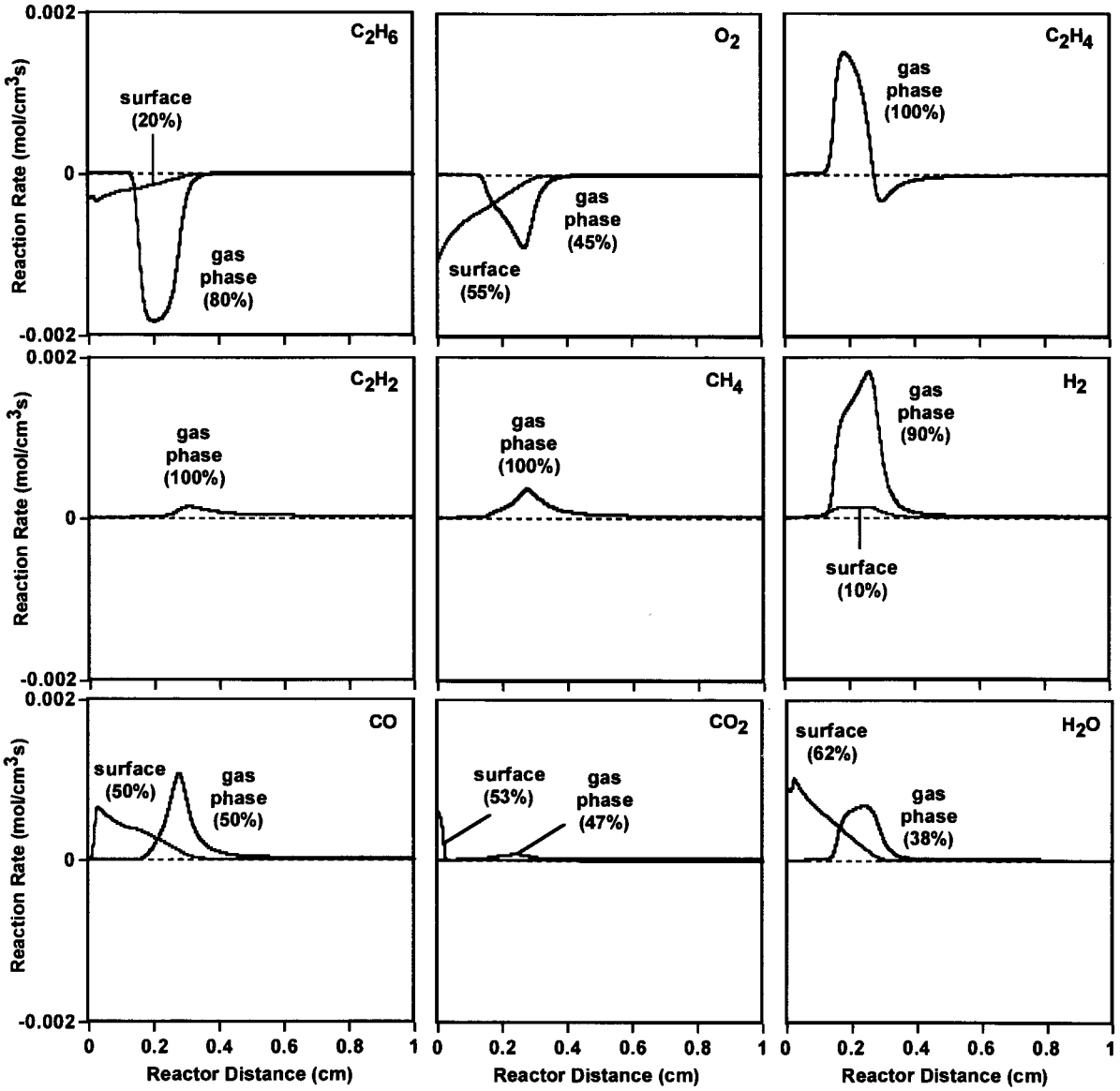

FIG. 6. Reaction rates as a function of actual monolith distance. The curves are calculations for $C_2H_6/O_2 = 1.2$ and 20% nitrogen dilution (2 slpm, 1.2 atm, 5.88 wt% Pt/α-Al_2O_3).

dioxide and water are produced first by surface-catalyzed steps and then in the gas phase; slightly larger amounts of CO_2 and H_2O are produced by surface-catalyzed steps than by gas-phase reactions. Overall, the results presented in Fig. 6 provide a clear measure of the significant participation of gas-phase chemistry at temperatures in excess of 850°C in the overall conversion of ethane in the catalytic monoliths.

5. CONCLUSIONS

The present analysis shows that gas-phase chemistry contributes significantly to the observed product distribution when ethane and oxygen are reacted over platinum-containing monoliths at temperatures in excess of 850°C. The analysis is based on well-established kinetics for gas-phase and surface reactions that have been previously reported in the literature. A key feature of the present analysis is the quantitative description of the heat evolution along the length of the monolith. The resulting temperature profile leads to a transition from surface reactions to gas-phase reactions as the conversion of the ethane proceeds. Our findings are consistent with an overall reaction scheme that begins with the oxidation of some of the ethane on the platinum surface. This sacrificial ethane leads to the formation of CO, CO_2, and H_2O in the front region of the monolith. The formation of these products causes a substantial temperature increase that drives the dehydrogenation of

ethane to ethylene in the gas phase. If the temperature is sufficiently high, some of this ethylene can further dehydrogenate to acetylene. Despite the endothermicity of these dehydrogenation reactions, the reactor temperature may continue to rise. This is because the heat needed by these reactions is supplied by concurrent nonselective exothermic gas-phase reactions that form additional CO and H_2O.

According to the present analysis, therefore, the main features of the oxidative dehydrogenation of ethane on platinum-containing monoliths can be understood in terms of a sequential process in which exothermic surface oxidation reactions are followed by a combination of endothermic and exothermic gas-phase reactions. There are large temperature gradients in the vicinity of the reaction front. The rapid rise in temperature along the monolith leads to the nearly exclusive formation of ethylene (and acetylene) via gas-phase homogeneous reactions. The role of the catalyst is therefore to initiate reactions that supply the heat for the subsequent gas-phase reactions.

ACKNOWLEDGMENTS

The authors thank Dr. Anthony M. Dean for helpful discussions and guidance in the use of gas-phase reaction mechanisms and D. W. Flick (University of Delaware) for the contribution in the generation of the experimental data used here.

REFERENCES

1. Hickman, D. A., and Schmidt, L. D., *J. Catal.* **138**, 267 (1992).
2. Hickman, D. A., and Schmidt, L. D., *AIChE J.* **39**, 1164 (1993).
3. Hickman, D. A., and Schmidt, L. D., *Science* **259**, 343 (1993).
4. Huff, M. C., and Schmidt, L. D., *J. Phys. Chem*. **97**, 11815 (1993).
5. Huff, M. C., and Schmidt, L. D., *AIChE J.* **42**, 3484 (1996).
6. Ostwald, W., *Chem. Zeitung* **47**, 457 (1903).
7. Dixon, J. K., and Longfield, J. E., *in* "Catalysis" (P. H. Emmet, Ed.), Vol. VII, pp. 281–302. Reinhold, New York, 1960.
8. Dean, A. M., *J. Phys. Chem*. **89**, 4600 (1985).
9. Dean, A. M., *J. Phys. Chem*. **94**, 1432 (1990).
10. Mims, C. A., Mauti, R., Dean, A. M., and Rose, K. D., *J. Phys. Chem*. **98**, 13357 (1994).
11. Witt, P. M., and Schmidt, L. D., *J. Catal.* **163**, 465 (1996).
12. Flick, D. W., and Huff, M. C., *Catal. Lett.* **47**, 91 (1997).
13. Androulakis, I. P., and Reyes, S. C., *AIChE J.* **45**, 860 (1999).
14. Kee, R. J., Rupley, F. M., and Miller, J. A., Sandia National Laboratories, Report SAND89-8009 (1990).
15. Brenan, K. E., Campbell, S. L., and Petzold, L. R., "SIAM Series in Applied Mathematics." Soc. for Industr. & Appl. Math., Philadelphia, 1996.
16. NAG Fortran Library, The Numerical Algorithm Group, Mark 17, (September 1995).